We are IntechOpen,
the world's leading publisher of
Open Access books
Built by scientists, for scientists

6,900
Open access books available

186,000
International authors and editors

200M
Downloads

Our authors are among the

154
Countries delivered to

TOP 1%
most cited scientists

12.2%
Contributors from top 500 universities

CLARIVATE ANALYTICS
BOOK CITATION INDEX
INDEXED

WEB OF SCIENCE™

Selection of our books indexed in the Book Citation Index
in Web of Science™ Core Collection (BKCI)

Interested in publishing with us?
Contact book.department@intechopen.com

Geometrical Exploration of Quantum Games

David Schneider

Additional information is available at the end of the chapter

http://dx.doi.org/10.5772/53931

1. Introduction

With nearly one decade of life, the theory of quantum games has nowadays become a very reach and prolific field of research. Multiplayer and multistrategy setups, a quantum approach to Evolutionary Game Theory, quantum game-like simulations of market phenomena, quantum duels, the effect of decoherence and noise during the implementation of a quantum game, are just some of the many scenarios where the quantum aspects of games were analyzed [2–4, 6, 7, 11–13, 16–18, 23]. Here we do not attempt to review the vast universe of quantum game theory, but just to give a comprehensive and didactic introduction to the pioneering work of Eisert [5]. This introduction will allow us to expose a recent approach developed to geometrically understand quantum games [20, 21], which represents the main focus this chapter. For a complete review of quantum games, we refer the reader to [9].

The theory of quantum games started in 1999 with the seminal papers by Meyer [15] and Eisert [5]. As usual, the first question that should be addressed is: why quantizing games? In their paper of 1999 , Eisert et at. outline the main reasons which make game theory a suitable framework for quantization. The first motivation relies on the probabilistic nature of the theory of games. Having a probabilistic background, it turns out to be natural an extension of game theory into the quantum probability domain. Moreover, as a game can be expressed as a setup where players exchange information with a 'referee', it becomes a perfect model to study quantum information. Finally, in [24] it was shown that the problem of the Optimal Cloning can be expressed in terms of a strategic game.

2. Eisert's quantum games

As Eisert's work relies on the quantization of the Prisoner's dilemma, we will devote a few lines to describe the features of this game (for a further description, see [10]). The Prisoner's dilemma is a standard example of a non-zero sum game, and it involves two parties, Alice (A) and Bob (B), who have to choose among the options 'cooperate' (C) and 'defect' (D). According to the decisions that the players make, they receive a payoff (see table 1). The dilemma arises from the fact that, although rational reasoning forces both players to defect, mutual cooperation represents a much better option for them. In game theory, these

two outcomes of the game, 'defect-defect' and 'cooperate-cooperate', are referred as Nash Equilibrium (NE) and Pareto Optimal (PO), respectively, and the fact that they can not be reached simultaneously, should be regarded as the theoretical origin of the conflict.

	Bob: C	Bob: D
Alice: C	$(3,3)$	$(0,5)$
Alice: D	$(5,0)$	$(1,1)$

Table 1. Bi-matrix representation of the Prisoner's dilemma. The first entry corresponds to the payoff of Alice, and the second entry to the payoff of Bob.

To understand the main ideas behind Eisert's theory, it is necessary to introduce mixed strategies. In a mixed strategy game, players do not decide which strategy they are going to play, but have the freedom to chose a probability distribution for the available strategies. For instance, in a 2×2 game like the Prisoner's dilemma, players can choose a value for a parameter p to be the probability for the strategy D. Accordingly, the set of strategies for Alice becomes a random variable with a Bernoulli distribution with parameter $p_A \in [0,1]$. Namely,

$$S_A \sim B(p_A), \quad \text{with } P^A(S_A) = \begin{cases} 1 - p_A & S_A = C \\ p_A & S_A = D \end{cases} \tag{1}$$

and the same for Bob. As the strategies are now probabilistic, the goal of the players is to maximize the mean value of the payoff function calculated over all possibles outcomes of the game, which for Alice reads

$$\bar{\$}_A(p_A, p_B) = \sum_{S_A, S_B} \$_A(S_A, S_B) P(S_A, S_B) \tag{2}$$

$$= \sum_{S_A, S_B} \$_A(S_A, S_B) P^A(S_A) P^B(S_B)$$

Nash equilibria are defined in an equivalent manner as in the pure strategy game, namely, as the vector $(p_A^*, p_B^*) \in [0,1]^{\otimes 2}$ such that

$$\bar{\$}_A(p_A^*, p_B^*) \geq \bar{\$}_A(p_A, p_B^*) \quad \forall p_A \in [0,1] \tag{3}$$
$$\bar{\$}_B(p_A^*, p_B^*) \geq \bar{\$}_B(p_A^*, p_B) \quad \forall p_B \in [0,1]$$

For instance, for the Prisoner's dilemma the mean value of the payoff function is given by $\bar{\$}_A(p_A, p_B) = 3 + 2p_A - 3p_B - p_A p_B$, and the game accounts for the single NE $(p_A^*, p_B^*) = (1,1)$, which corresponds to the joined strategy (D,D) of the pure strategy game. A more interesting example concerns the Chicken game, which can be represented by the following bi-matrix

The mean value of the payoff function reads now $\bar{\$}_A(p_A, p_B) = 3 + 2p_A - p_B - 3p_A p_B$, and the NE are represented by the pure strategies $(p_A^*, p_B^*) = (1,0)$ and $(p_A^{**}, p_B^{**}) = (0,1)$, corresponding to (D,C) and (C,D) respectively, and the mixed strategy NE $(p_A^{***}, p_B^{***}) = (2/3, 2/3)$.

In order to introduce Eisert's scheme for quantizing games, it is worth to give a formal framework to the mixed strategy games. This can be done by considering a vector

	Bob: C	Bob: D
Alice: C	(3,3)	(2,5)
Alice: D	(5,2)	(1,1)

Table 2. Bi-matrix representation of the Chicken game.

representing the probabilities for the players to chose the available strategies. For instance, for Alice this vector reads

$$x_A = \begin{bmatrix} P^A(C) \\ P^A(D) \end{bmatrix} = \begin{bmatrix} 1 - p_A \\ p_A \end{bmatrix} \tag{4}$$

and it is defined in a vector space spanned by the canonical vectors

$$p_A = 0 \sim \begin{bmatrix} 1 \\ 0 \end{bmatrix} \quad p_A = 1 \sim \begin{bmatrix} 0 \\ 1 \end{bmatrix} \tag{5}$$

The strategies are represented by stochastic matrices acting on the initial 1-player state $p_A = 0$,

$$M_A = \begin{bmatrix} 1 - p_A & p_A \\ p_A & 1 - p_A \end{bmatrix} \tag{6}$$

so that

$$x_A = M_A \cdot \begin{bmatrix} 1 \\ 0 \end{bmatrix} \tag{7}$$

With this construction, the action of the players can be regarded as a stochastic process in which the players receive a biased coin (with all the probability in the side "C"), and change the probabilities by applying the stochastic matrix to the initial vector. For example, the pure strategies are represented by the matrices

$$\tilde{C} = M_A(0) = \begin{bmatrix} 1 & 0 \\ 0 & 1 \end{bmatrix} \quad \text{and} \quad \tilde{D} = M_A(1) = \begin{bmatrix} 0 & 1 \\ 1 & 0 \end{bmatrix} \tag{8}$$

Finally, the payoff assignment can be defined through a matrix in the 2-players space

$$\mathbb{S}_A = \begin{bmatrix} \$_A(C,C) & 0 & 0 & 0 \\ 0 & \$_A(C,D) & 0 & 0 \\ 0 & 0 & \$_A(D,C) & 0 \\ 0 & 0 & 0 & \$_A(D,D) \end{bmatrix} \tag{9}$$

so that the average payoff is computed as the trace of $\mathbb{S}_A$ times the state of probabilities of the players $\rho = x_A \otimes x_B$.

$$\text{Tr}[\mathbb{S}_A . x_A \otimes x_B] = \bar{\$}_A(p_A, p_B) \tag{10}$$

The procedure of quantization is now straightforward, as the probabilities need to be simply replaced by amplitude probabilities and the stochastic matrices by unitary operators,

- $x \to |x\rangle = a|0\rangle + b|1\rangle$ ($|a|^2 + |b|^2 = 1$), initial state: $|0\rangle$

- $M \to \hat{U}(\theta, \phi, \eta) \sim \begin{bmatrix} e^{i\phi}\cos(\theta/2) & e^{i\eta}\sin(\theta/2) \\ -e^{-i\eta}\sin(\theta/2) & e^{-i\phi}\cos(\theta/2) \end{bmatrix}$

After quantization, the pure strategies C and D of the classical game become the identity and the spin flip operators, respectively,

$$\hat{C} = \hat{U}(0,0,0) \sim \begin{bmatrix} 1 & 0 \\ 0 & 1 \end{bmatrix} \text{ and } \hat{D} = \hat{U}(\pi,0,0) \sim \begin{bmatrix} 0 & 1 \\ -1 & 0 \end{bmatrix} \tag{11}$$

The corresponding payoff assignment is the operator whose matrix elements are those of equation 9

$$\hat{\$}_A = \$_A(C,C) \, |00\rangle \, \langle 00| + \$_A(C,D) \, |01\rangle \, \langle 01| \\ + \$_A(D,C) \, |10\rangle \, \langle 10| + \$_A(D,D) \, |11\rangle \, \langle 11| \tag{12}$$

so that

$$\text{Tr}[\hat{\$}_A \, |\psi_f\rangle \, \langle \psi_f|] = \langle \psi_f| \, \hat{\$}_A \, |\psi_f\rangle \tag{13}$$

with $|\psi_f\rangle = \hat{U}_A \otimes \hat{U}_B \, |00\rangle$.

There are two important things to be pointed out. First, the procedure relies on an usual formalism for quantization, so it represents an very acceptable framework to study quantum phenomena. And second, the new game entitles the classical game, so the latter can be reobtained as its classical limit. As a matter of fact, by the identification $p = \sin^2(\theta/2)$ it turns out that both Eisert's quantum game and the mixed strategy classical game are the same. This fact makes necessary to include any new ingredient in the theory. This new ingredient, with no classical counterpart, is the entanglement between the states of the two players represented by the unitary operator $\hat{J}(\gamma) = \exp(i\gamma D \otimes D/2)$.

Figure 1 outlines the circuital representation of Eisert's protocol. The final state $|\psi_f\rangle = \hat{J}^\dagger(U_A \otimes U_B)\hat{J} \, |00\rangle$ is the state by means of which the expectation value of the operator $\hat{\$}_A$ is calculated.
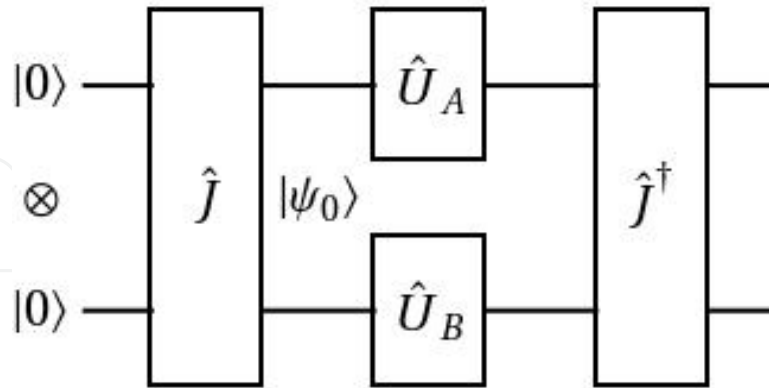

Figure 1. Eisert's quantization protocol for 2-player games.

Eisert's results relies on the so called two-parameter operator

$$\hat{U}(\theta,\phi,\eta) \sim \begin{bmatrix} e^{i\phi}\cos(\theta/2) & \sin(\theta/2) \\ -\sin(\theta/2) & e^{-i\phi}\cos(\theta/2) \end{bmatrix} \tag{14}$$

The authors argue that it proves to be sufficient to restrict the space of strategies to this set of unitary operators, with $\theta \in [0, \pi]$ and $\phi \in [0, \pi/2]$. For $\phi = 0$ the game again reduces to the mixed strategy Prisoner's dilemma, meaning a unique NE for the pure joined strategy 'defect-defect'. However, the extra degree of freedom given by the parameter ϕ makes the game behave differently. Eisert et al. choose $\hat{J} = \exp(i\pi \hat{D} \otimes \hat{D}/4)$, which makes the initial state maximal entangled, and show that 'defect-defect' ceases now to be a NE. For instance, the players can improve by taking the strategy

$$\hat{Q} \equiv \hat{U}(0, \pi/2) = \begin{bmatrix} i & 0 \\ 0 & -i \end{bmatrix}. \tag{15}$$

By computing the payoff expectation value for Alice [1], it turns out that $\$_A(\hat{D}, \hat{Q}) = 5$, meaning that

$$\$_A(\hat{D}, \hat{D}) < \$_A(\hat{Q}, \hat{D}). \tag{16}$$

The main result of [5], however, concerns the emergence of a new NE given by the outcome '$\hat{Q}-\hat{Q}$', for which $\$_A = \$_B = 3$. This solution fulfills not only the NE condition, provided that

$$\$_A(\hat{U}(\theta, \phi), \hat{Q}) = \$_B(\hat{Q}, \hat{U}(\theta, \phi)) = \cos^2(\theta/2)(3\sin^2\phi + \cos^2\phi) \leq 3, \tag{17}$$

but it is also an outcome of the game which rewards Alice and Bob as good as the mutual cooperation (Pareto Optimal condition). In that sense, this is a version of the game that on one hand encompasses the classical Prisoner's dilemma, and on the other hand has the intriguing feature of making the players able to perform an optimal decision.

3. A periodic point-based method to analyze Nash equilibria in Eisert's quantum games

In this section, we introduce a periodic point-based method designed to explore the strategy space in order to identify those strategies which fulfill the NE condition. The general problem concerns two functions $f_A(x, y)$ and $f_B(x, y)$ such that $f_B(x, y) = f_A(y, x)$, and every point (x^*, y^*) satisfying the generalized NE definition,

$$f_A(x^*, y^*) \geq f_A(x, y^*) \quad \forall x \tag{18}$$
$$f_B(x^*, y^*) \geq f_B(x^*, y) \quad \forall y. \tag{19}$$

The map associated to the game is defined as the (eventually multivalued) function that, for a given value of the second argument of $f_A(x, y)$, picks the (eventually multiple) value of the first argument which makes $f_A(x, y)$ maximal[2]. Specifically,

$$M(y) = x, \tag{20}$$

for every x satisfying

$$f_A(x, y) \geq f_A(x', y) \quad \forall x'. \tag{21}$$

Following the previous definition, a pair (x^*, y^*) satisfying equation 18 must be obviously a pair for which

$$M(y^*) = x^*. \tag{22}$$

---

[1] From now on, we will use the symbol '$\$$' to refer to the expectation value $\langle \hat{\$} \rangle$.

[2] In game theory language, this map is called 'best response correspondence'.

Equation 19, instead, can be rearranged by means of the symmetry relationship of the two functions. This procedure leads to an equivalent equation as the previous one, but with the roles of x^* and y^* inverted,

$$M(x^*) = y^*. \tag{23}$$

By simply applying the map to both sides of 22 and combining with equation 23, one obtains

$$M^2(y^*) = y^*. \tag{24}$$

According to equation 24, all NE of the game defined by the functions $f_A(x, y)$ and $f_B(x, y)$ can be extracted from the 2-periodic points of M, and are of the form $(y^*, M(y^*))$.

For $M(y^*) = y^*$, y^* turns out to be a fixed point of M. We will refer to this solution of the form (y^*, y^*) as a fixed point NE, and to those for which $M(y^*) \neq y^*$ as 2-cycle NE.

3.1. A simple example

As the classical Prisoner's dilemma (even in its mixed-strategy version) accounts for a fixed point NE only, it is not a suitable example to illustrate the method implementation. The simplest example which shows how the method picks fixed point and 2-cycle NE concerns the mixed-strategy version of the Chicken game, derived from the bi-matrix of table 2.

Renaming $p \equiv p_A$ and $q \equiv p_B$, the mean value of the payoff function reads $\bar{\$}_A(p, q) = 3 + 2p - q - 3pq$. The map M is therefore an eventually multivalued function of Bob's mixed strategy q[3].
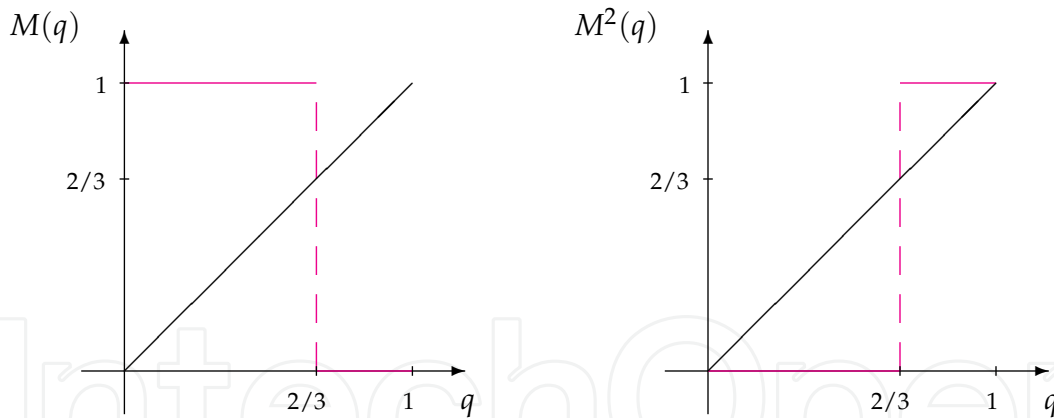

Figure 2. First (left) and second (right) iterations of the maximization map for the mixed-strategy Chicken game. Attached to each plot, a line at 45° which intersects each function at its fixed points. The point $q = 2/3$ is mapped both under M and M^2 into the whole interval $[0, 1]$ (dashed lines).

Figure 2 illustrates the shape of the first and the second iterations of the map M. A straight line at 45° is attached to each plot to graphically identify the fixed points and the 2-period orbits of M, which in general are obtained from the plot of M^2. The latter map has three fixed points, namely, $q_1^* = 0$, $q_2^* = 2/3$ and $q_3^* = 1$. The corresponding NE are deduced by taking each of these fixed points and computing the corresponding value $M(q^*)$. Proceeding

---

[3] The maximization map associated to the mixed-strategy classical Prisoner's dilemma is the constant and idempotent function $M(q) = M^2(q) = 1 \; \forall q \in [0, 1]$, as can be deduced from Alice's payoff function $\bar{\$}_A(p, q) = 3 + 2p - 3q - pq$. Hence, the game has not periodic orbits except the fixed point $q = 1$. This fact implies a sole NE for $p = q = 1$, namely, for the pure joined strategy 'defect-defect'.

like this, one immediately recognizes the two NE related to the pure strategy game, given by $(p_1^*, q_1^*) = (0, 1)$ and $(p_3^*, q_3^*) = (1, 0)$. According to our previous nomenclature, these are 2-cycle NE. The remaining fixed point of M^2 is also a fixed point of M ($p_2^* = q_2^* = 2/3$), and it corresponds therefore to a fixed point NE. Of course, this NE is not present in the pure strategy game.

3.2. Topological aspects of Eisert's game's maps

Now the mechanism for identifying NE is described, our next goal is to extend it for the case of the 2-parameter quantum Prisoner's dilemma. For that purpose, we consider the maximization map for that problem, obtained from equation 20 by taking $x = \hat{U}(\theta', \phi')$, $y = \hat{U}(\theta'', \phi'')$, and $f_A = \$_A$. Accordingly, we write now

$$M(\hat{U}(\theta'', \phi'')) = \hat{U}(\theta', \phi'), \tag{25}$$

for every $\hat{U}(\theta', \phi')$ satisfying

$$\$_A(\hat{U}(\theta', \phi'), \hat{U}(\theta'', \phi'')) \geq \$_A(\hat{U}(\theta''', \phi'''), \hat{U}(\theta'', \phi'')) \quad \forall \hat{U}(\theta''', \phi''').$$

Following the steps of Eisert's protocol, one gets the following expression for Alice's payoff function,

$$\$_A(\hat{U}(\theta', \phi'), \hat{U}(\theta'', \phi'')) = 3[\cos(\phi' + \phi'') \cos(\theta'/2) \cos(\theta''/2)]^2$$
$$+ 5\left[\sin(\phi') \cos(\theta'/2) \sin(\theta''/2) - \cos(\phi'') \cos(\theta''/2) \sin(\theta'/2)\right]^2 \tag{26}$$
$$+ \left[\sin(\phi' + \phi'') \cos(\theta'/2) \cos(\theta''/2) + \sin(\theta'/2) \sin(\theta''/2)\right]^2.$$

By inserting this function in the definition above, however, it is not difficult to check that for M to be a well defined map, we are forced to take in to account the following extended strategy set,

$$S = \{U(\theta, \phi)| -\pi \leq \theta \leq \pi \text{ and } -\pi/2 \leq \phi \leq \pi/2\}. \tag{27}$$

The latter definition ensures that every point in the M domain is mapped into the same region, namely, that the map M is actually an endomorphism[4]. As it is usual for bidimensional maps, we will make a planar representation of the M domain. This representation deserves however a detailed explanation, because it will be crucial for the analysis of the periodic points of the map. We stress that the map given by equations 25, 26 and 27 is defined on a compact surface which can not be continuously embedded in a tridimensional manifold. This special surface is called projective plane, and it is central in 2-dimensional algebraic topology [14]. The construction of a projective plane follows a square's edges identification scheme similar to that employed to construct a torus or a sphere (see figure 3). As in the case of a torus, the scheme follows an identification of opposite edges, however the edges are inverted before the identification. The important fact is that this inversion makes it possible to repeat the construction starting from a 2-edges-polygon, as it is also the case in the construction of a sphere. Nevertheless, as the edges have to be also inverted in the 2-edges diagram of the projective plane, the 'North' and 'South' poles merge ultimately into the same point[5].

---

[4] Moreover, the region in the parameter space defined by means the set of strategies S turns out to be the smallest region which guaranties the endomorphic character of M. Of course, this set encompass the set of strategies defined in [5], but it is not however a redundant set.

[5] Equivalently, a projective plane can be constructed starting from a square and generating a Möbius strip. If in a second step we map the (single) edge of the Möbius strip into one point (as we would map the two edges of a cylinder into the two points that would result in the poles of a sphere), the compact surface we obtain is actually a projective plane.
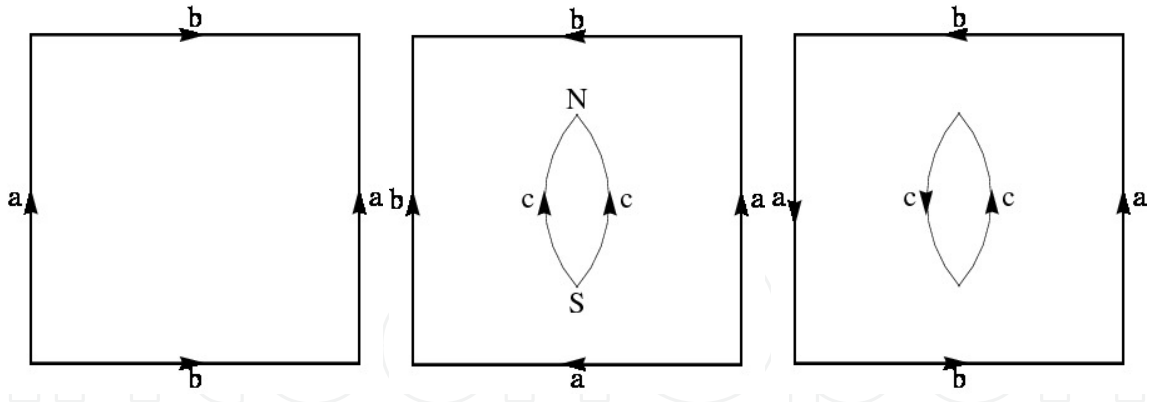
Figure 3. The square's edges identification scheme for the construction of a torus (left), a sphere (middle), and a projective plane (right). Attached to the latter two pictures, an equivalent construction performed with 2-edges-polygons to emphasizes the fact that, when the procedure is accomplished for a projective plane, the poles of the sphere (denoted by N and S) merge into the same point.

Following an analogy with the planar representation of the earth surface, and regarding θ and ϕ as the latitudes and longitudes, respectively, we may say that the map M is defined on a domain whose extreme longitudes ($\phi = \pm\pi/2$) have to be identified after a reflexion by means the equator ($\theta = 0$), so that the extreme latitudes (the 'lines' representing the poles, $\theta = \pm\pi$) result in two representations of the same point.

We are now in the position to explain the numerical exploration of the map of equation 25. However the topological aspects of the map domain are more complicated, there are many features in the analysis analogous to those outlined for the very simple example of the the previous section. When possible, we will refer to those similarities to make the picture clearer. Figure 4 depicts the first and second iterations under M of the projective plane first quadrant (except for the line segment $\phi = \tilde{\phi} = \arccos(1/5)/2$. Five line segments for five different values of the parameter ϕ (with $\theta \in [0, \pi]$) are mapped under M into five different curves at the second quadrant, respectively. The latter curves are in turn mapped into five different curves at the fourth quadrant. The following remarks summarize the overall behavior of the map,

- For $\phi < \tilde{\phi} = \arccos(1/5)/2$, the map image of every line segment $\phi = \phi_0$ starts at $\theta = \pi$ (a piece of the projective plane pole), whereas for $\phi > \tilde{\phi}$, the map images start at the points with coordinates $\phi = -\phi_0$, $\theta = 0$.

- All map images of the line segments $\phi = \phi_0$ finish at the point with coordinates $\phi = -\pi/2$, $\theta = 0$ (which is the same as that with coordinates $\phi = \pi/2$, $\theta = 0$).

- For $\phi < \tilde{\phi}$, the second iterations of the line segments $\phi = \phi_0$ start and finish at the point with coordinates $\phi = \pi/2$, $\theta = 0$; whereas for $\phi > \tilde{\phi}$ the corresponding iterations start at the points with coordinates $\phi = \phi_0$, $\theta = 0$, and finish at the points with coordinates $\phi = \pi/2$, $\theta = 0$.

- As ϕ goes to $\pi/2$, the map images of the line segments $\phi = \phi_0$ converge to the point with coordinates $\phi = -\pi/2$, $\theta = 0$, whereas the second iterations converge to the point with coordinates $\phi = \pi/2$, $\theta = 0$ (which is the same as the previous one).

In figure 5, we sketch the behavior of the map for points on the line segment $\phi = \tilde{\phi}$. In the open interval $(0, \pi]$, the segment in the first quadrant maps into the solid curve at the second
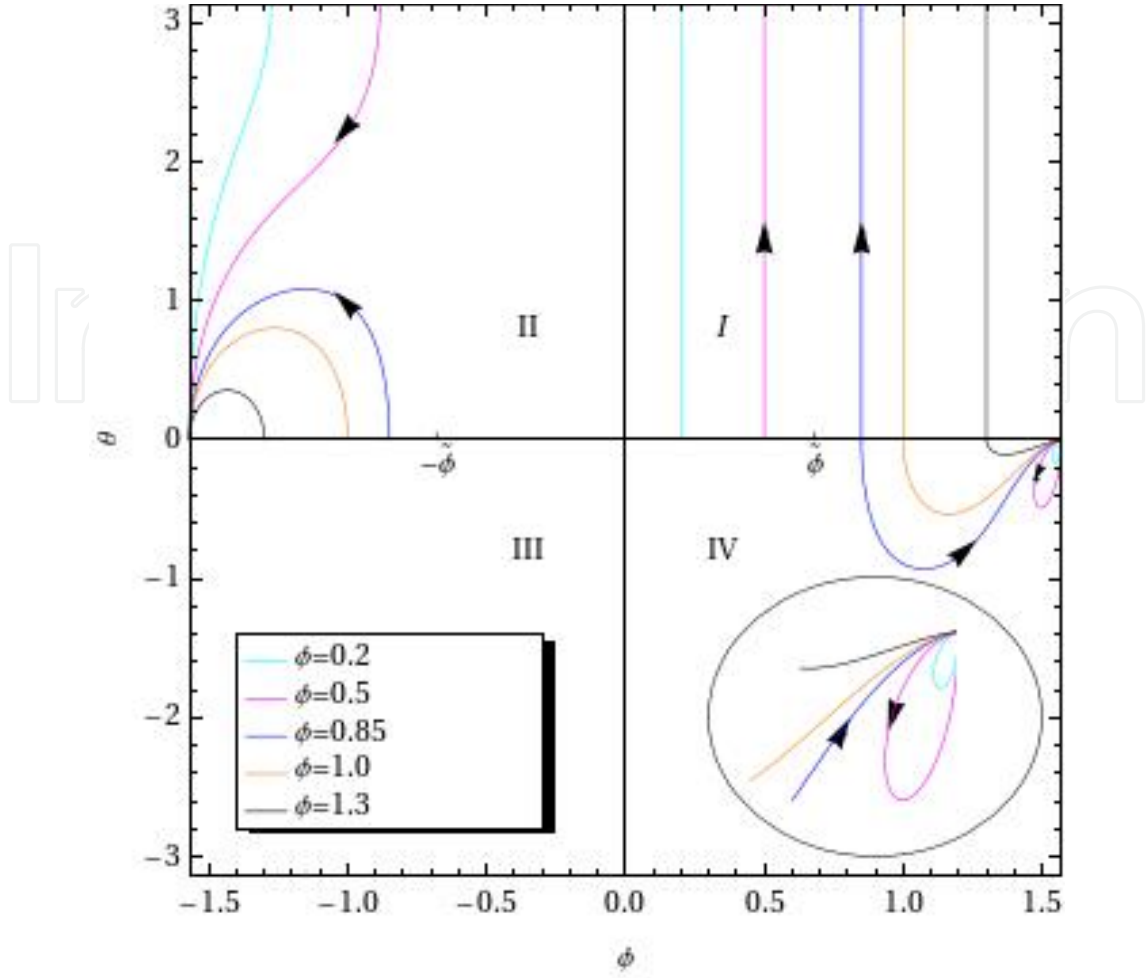
Figure 4. For the first quadrant of the extended strategy set, the first and second iterations of the maximization map of the 2-parameter quantum Prisoner's dilemma. The line segments corresponding to different values of the parameter ϕ are mapped into several curves at the second quadrant, which are in turn mapped into the corresponding curves at the fourth quadrant. $\tilde{\phi} = \arccos(1/5)/2 \simeq 0.685$.

quadrant in a similar fashion as for the remaining values of ϕ. However, for $\theta = 0$ the map becomes a multivalued function having its image at all points on the dotted line $\phi = -\tilde{\phi}$, with $\theta \in [-\pi, \pi]$. This behavior is exactly the same as for the strategy $q = 2/3$ in the mixed strategy Chicken game.

Finally, the second iteration of the map for the line segment $\phi = \tilde{\phi}$ at the first quadrant is depicted in figure 6. The black-solid curve at the second quadrant corresponds to the first iteration for $\theta \in (0, \pi]$ (compare with figure 5), which is mapped into the black-solid curve at the fourth quadrant. We split the first iteration of the point with coordinates $\phi = \tilde{\phi}$, $\theta = 0$ (namely, the dotted line $\phi = -\tilde{\phi}$ of figure 5) in three parts: the green segment $\theta > 0$, which is mapped into the green curve at the first quadrant, the red segment $\theta < 0$, which is mapped into the red curve at the fourth quadrant, and the point $\theta = 0$, which again makes the map a multivalued function, having its image in all points on the dotted line $\phi = \tilde{\phi}$, with $\theta \in [-\pi, \pi]$. This is again comparable with the behavior of the mixed strategy $q = 2/3$ in the previous section, when iterated for a second time.
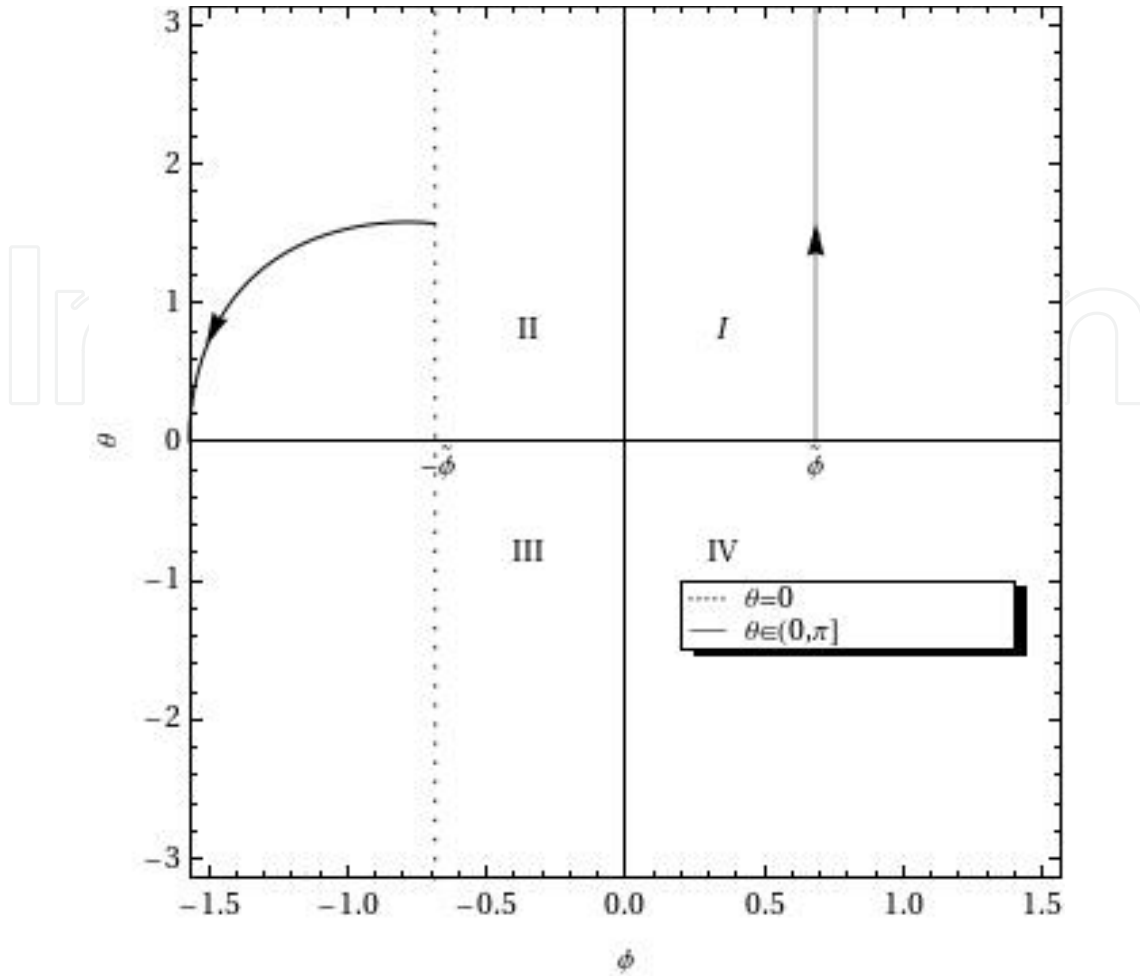
Figure 5. First iteration of the line segment $\phi = \tilde{\phi}$ (with $\theta \in [0, \pi]$) for the 2-parameter quantum Prisoner's dilemma. The point with coordinates $\theta = 0$, $\phi = \tilde{\phi}$ is mapped into the entire (dotted) line $\phi = -\tilde{\phi}$.

According to the previous statements, only points with coordinates $\theta = 0$, $\tilde{\phi} \le \phi \le \pi/2$ represent 2-periodic points of the map. By repeating the analysis for the fourth quadrant one obtains exactly the same outcome, whereas for the second and third quadrant the 2-periodic points turn out to be represented by the points with coordinates $\theta = 0$, $-\pi/2 \le \phi \le -\tilde{\phi}$.

We can summarize the results of this section by arguing that the 2-periodic orbits of the map related to the 2-parameter quantum Prisoner's dilemma, in its extended strategy version, lay on the projective plane equator $\theta = 0$, excluding those points with coordinates $|\phi| < \tilde{\phi}$. Moreover, these periodic points are such that $M(\theta, \phi) = (\theta, -\phi)$. Finally, as coordinates $\theta = 0$, $\phi = -\pi/2$, and $\theta = 0$, $\phi = \pi/2$ represent the same point in the projective plane, this point turns out to be actually a fixed point of the map.

3.3. Nash equilibria in the extended strategy 2-parameter quantum Prisoner's dilemma

In what follows, we will check the connection between the periodic points of the map discussed above and the NE of the quantum game. As it was already mentioned, a joined
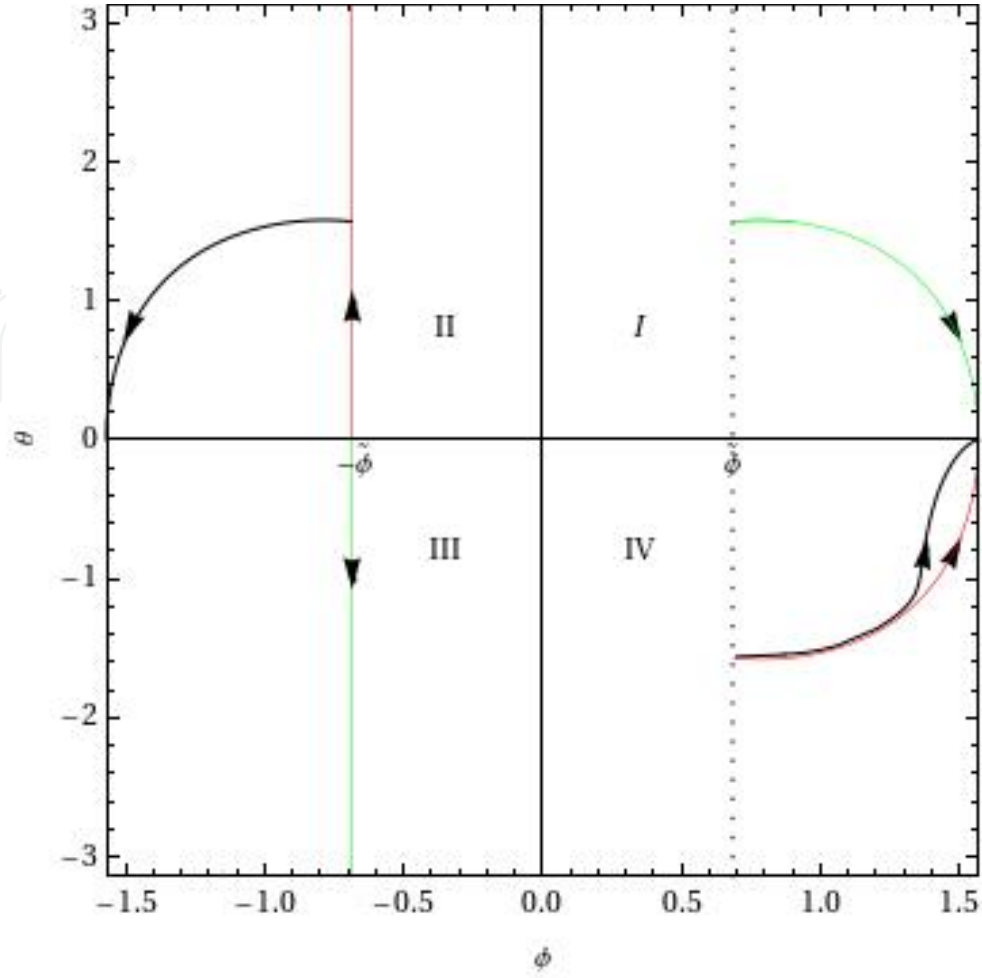
Figure 6. Second iteration of the line segment $\phi = \tilde{\phi}$ (with $\theta \in [0, \pi]$). The solid-black curve at the second quadrant (map image of the line segment $\phi = \tilde{\phi}$, with $\theta \in (0, \pi]$) is mapped into the solid-black curve at the fourth quadrant. The first iteration of the point with coordinates $\phi = \tilde{\phi}$, $\theta = 0$ (represented by the red and green line segments at the second and third quadrants) is mapped into the red and green curves at the fourth and first quadrants. Finally, the point with coordinates $\phi = -\tilde{\phi}$, $\theta = 0$, belongs also to the image under M of the point with coordinates $\phi = \tilde{\phi}$, $\theta = 0$, and it is mapped into the entire line $\phi = \tilde{\phi}$.

strategy fulfilling NE conditions is related to both periodic points in a 2-periodic orbit (namely, to one particular periodic point, and to its iteration). So let us define the quantum strategies

$$\hat{R}_{\pm} \equiv \hat{U}(0, \pm\alpha)$$

with $\alpha \in [0, \pi/2]$, and consider the functions defined as follows:

$$f_A^{\pm}(\theta, \phi) \equiv \$_A(\hat{R}_{\mp}, \hat{R}_{\pm}) - \$_A(\hat{U}(\theta, \phi), \hat{R}_{\pm}).$$

By replacing 26 in the previous definition, and after some manipulations, one obtains

$$f_A^{\pm}(\theta, \phi) = 3 - \cos(\theta/2)^2 [2 + \cos(2(\alpha \pm \phi))] - 5\cos(\alpha)^2 \sin(\theta/2)^2. \tag{28}$$

Figure 7 shows the contours of $f_A^+(\theta, \phi)$ for different values of the parameter α. It turns out that the this function is positive-semidefinite whenever $\tilde{\phi} \leq \alpha \leq \pi/2$, and it has positive and negative regions for $0 \leq \alpha < \tilde{\phi}$. In addition, equation 28 implies that $f_A^+(\cdot, \phi) = f_A^-(\cdot, -\phi)$,
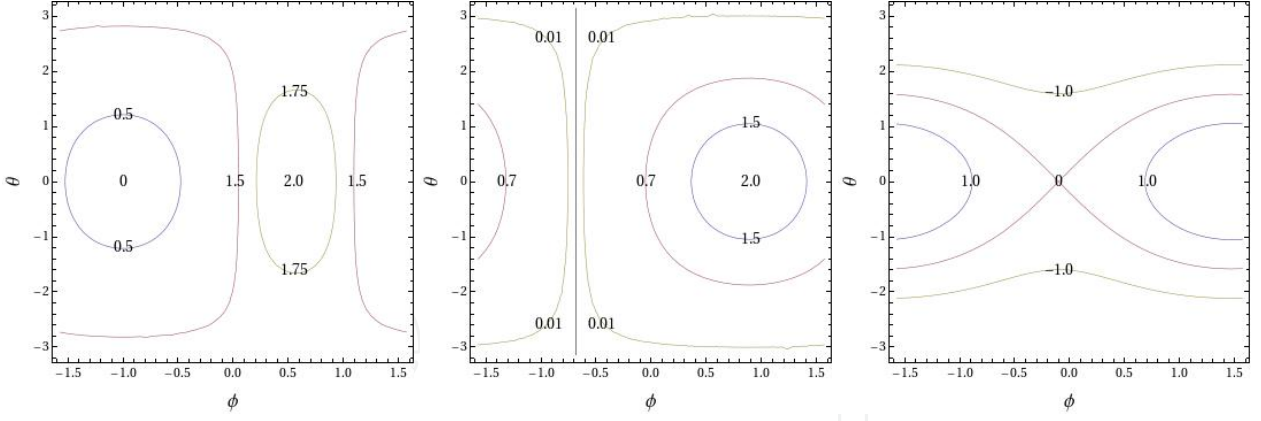
Figure 7. Contours of the function $f_A^+(\theta, \phi)$ for different values of the parameter α. Left: $\alpha = 1$, middle: $\alpha = \tilde{\phi}$, right: $\alpha = 0.1$.

meaning that the previous statements applies in the same way for the function f_A^-. Now, according to the symmetry relationship between $\$_A$ and $\$_B$, we can rewrite equation 28 as follows,

$$f_A^+(\theta', \phi') = \$_A(\hat{R}_-, \hat{R}_+) - \$_A(\hat{U}(\theta', \phi'), \hat{R}_+)$$
$$f_A^-(\theta'', \phi'') = \$_B(\hat{R}_-, \hat{R}_+) - \$_B(\hat{R}_-, \hat{U}(\theta'', \phi'')).$$

The latter observation, and the fact that f_A^+ and f_A^- behave with the parameter α as discussed above, imply in conclusion that

$$\$_A(\hat{R}_-, \hat{R}_+) \geq \$_A(\hat{U}(\theta', \phi'), \hat{R}_+) \quad \forall(\theta', \phi')$$
$$\$_B(\hat{R}_-, \hat{R}_+) \geq \$_B(\hat{R}_-, \hat{U}(\theta'', \phi'')) \quad \forall(\theta'', \phi'')$$

if and only if $\tilde{\phi} \leq \alpha \leq \pi/2$. Being the argument in the previous paragraphs symmetric under the interchange of the strategies $\hat{R}_+$ and $\hat{R}_-$, we assert that the outcomes of the game given by the joined strategies '$\hat{R}_- - \hat{R}_+$' and '$\hat{R}_+ - \hat{R}_-$' represent Nash Equilibria provided that $\tilde{\phi} \leq \alpha \leq \pi/2$. These Nash Equilibria are of diagonal type only in the case in which $\hat{R}_+$ and $\hat{R}_-$ coincide (up to a global phase), what happens for the special value $\alpha = \pi/2$. The latter strategy corresponds to the Eisert's operator $\hat{Q}$.

To give a possible interpretation for the NE observed in the extended strategy quantum Prisoner's dilemma, let consider the 2-player game given by the following bi-matrix

	Bob: $\hat{C}$	Bob: $\hat{D}$	Bob: $\hat{Q}$
Alice: $\hat{C}$	(3,3)	(0,5)	(1,1)
Alice: $\hat{D}$	(5,0)	(1,1)	(0,5)
Alice: $\hat{Q}$	(1,1)	(5,0)	(3,3)

where $\hat{C}$, $\hat{D}$ and $\hat{Q}$ are the quantum strategies of the Eisert's game. This reduced game, being different from the 2-parameter quantum Prisoner's dilemma, summarizes in a simple manner the ideas behind Eisert's result. Namely, if the strategy $\hat{Q}$ were not present, a possible agreement (to "C-ooperate") of the parties before they make their decisions would make no sense. As departing from the strategy $\hat{C}$ would keep improving their payoffs, the dilemma would persists as before the agreement. However, the table clearly shows that the situation is different if after the agreement they decide to "Q-ooperate" (namely, to simultaneously choose the strategy $\hat{Q}$). Now, they can not be further better off by departing from the agreement

solution (on the contrary, it would be a self destructive behavior). Of course, we have not said much up to this point, but just showed in a concise fashion what Eisert's new NE exactly means.

Now, we can follow a similar idea and construct a reduced game which extracts the features present in the extended strategy quantum game. This is accomplished by including two more strategies in the normal form, which mean the $\hat{R}_-$ and $\hat{R}_+$ strategies for some specific, but arbitrary, value $\tilde{\phi} \leq \alpha < \pi/2$. We choose for example the value $\alpha = \pi/4$.

	Bob: $\hat{C}$	Bob: $\hat{D}$	Bob: $\hat{Q}$	Bob: $\hat{R}_+$	Bob: $\hat{R}_-$
Alice: $\hat{C}$	(3,3)	(0,5)	(1,1)	(2,2)	(2,2)
Alice: $\hat{D}$	(5,0)	(1,1)	(0,5)	(2.5,2.5)	(2.5,2.5)
Alice: $\hat{Q}$	(1,1)	(5,0)	(3,3)	(2,2)	(2,2)
Alice: $\hat{R}_+$	(2,2)	(2.5,2.5)	(2,2)	(1,1)	(3,3)
Alice: $\hat{R}_-$	(2,2)	(2.5,2.5)	(2,2)	(3,3)	(1,1)

It is straightforward to check from the table above that the three solutions '$\hat{Q} - \hat{Q}$', '$\hat{R}_+ - \hat{R}_-$' and '$\hat{R}_- - \hat{R}_+$' behave in this 5-strategy game as optimal NE, exactly as '$\hat{Q} - \hat{Q}$' does in the 3-strategy game associated to the Eisert's quantum game. However, we stress here the importance of the previously mentioned agreement. That agreement is not usually included in the story of the Prisoner's dilemma (see for example [10]), although it does not change the nature of the game (at both the classical and quantum levels). However, in our extended strategy version of the quantum game that agreement is crucial because both players could otherwise destroy themselves not by defection, but just by ignorance (for example, they could play the strategy '$\hat{R}_+ - \hat{R}_+$' receiving a payoff of 1 each. Or any other combination of $\hat{Q}$, $\hat{R}_+$ and $\hat{R}_-$ different from the NE outcomes).

The following table is constructed just to show that for $|\alpha| < \tilde{\phi}$ (in this case we choose $\alpha = \pi/6$) '$\hat{R}_+ - \hat{R}_-$' and '$\hat{R}_- - \hat{R}_+$' do not fulfill the NE conditions, and hence the corresponding reduced game is not suitable to depict the features of the extended strategy quantum game.

	Bob: $\hat{C}$	Bob: $\hat{D}$	Bob: $\hat{Q}$	Bob: $\hat{R}_+$	Bob: $\hat{R}_-$
Alice: $\hat{C}$	(3,3)	(0,5)	(1,1)	(2.5,2.5)	(2.5,2.5)
Alice: $\hat{D}$	(5,0)	(1,1)	(0,5)	(3.75,1.25)	(3.75,1.25)
Alice: $\hat{Q}$	(1,1)	(5,0)	(3,3)	(1.5,1.5)	(1.5,1.5)
Alice: $\hat{R}_+$	(2.5,2.5)	(1.25,3.75)	(1.5,1.5)	(1,1)	(3,3)
Alice: $\hat{R}_-$	(2.5,2.5)	(1.25,3.75)	(1.5,1.5)	(3,3)	(1.5,1.5)

4. The periodic point method in different scenarios

The aim of this section is to explore how the periodic point method gives rise to different outcomes when applied to other 2×2 quantum games. For that purpose we extend the previous analysis to the Chicken game and to a symmetrized version of the Battle of the Sexes.

4.1. The extended strategy quantum Chicken game

A possible normal form of the Chicken game was given in section 3. As already mentioned, the mixed-strategy game has three NE, namely, the two NE of the pure strategy game and

a third NE represented by the outcome $p_A = p_B = 2/3$. Curiously, when applied to the quantum version of this game, the periodic point procedure gives rise to a similar picture as that of Figure 4. Line segments at constant values of ϕ in the first quadrant are mapped into curves at the second quadrant, which are in turn mapped into curves at the forth quadrant. Hence, the set of strategies of equation 27 should be considered again as the smallest space which guaranties the endomorphic behavior of M. Moreover, the first and second iterations of the first quadrant can be obtained after smooth deformations of the curves displayed in Figure 4, as well as the iterations of the remaining quadrants (not shown). The latter remarks imply that the maps associated to the quantum Chicken game and to the quantum Prisoner's dilemma are topological equivalent, so that the results outlined in section 3 are immediately applicable to the quantum Chicken game. The set of NE is again given by the joined strategies '$\hat{R}_+ - \hat{R}_-$' and '$\hat{R}_- - \hat{R}_+$' with $\tilde{\phi} \leq \alpha \leq \pi/2$ (for the new value $\tilde{\phi} = \arccos(-1/3)/2 \simeq 0.955$), and all these strategies are optimal in the sense of Eisert's solution $\hat{Q} - \hat{Q}$. It is interesting to observe that, even when both games (the Prisoner's dilemma and the Chicken) are totally different at the classical level, they show the same quantum behavior.

4.2. The extended strategy quantum symmetrized Battle of the Sexes

We finally present a symmetrized version of the Battle of the Sexes game. As the well known Battle of the Sexes, this game has two NE in its pure classical presentation and it faces both players to a problematic decision. However, the two NE are now located at the off-diagonal positions. The normal form of the game is given in the following bi-matrix[6] However the

	Bob: C	Bob: D
Alice: C	$(0,0)$	$(1,2)$
Alice: D	$(2,1)$	$(0,0)$

Table 3. Bi-matrix representation of the simmetrized Battle of the Sexes game.

payoff function of the mixed-strategy game is given now by $\bar{\$}_A = 2\,p_A + p_B - 3\,p_A\,p_B$, the corresponding 1-dimensional map is exactly the same as that of the mixed-strategy Chicken game, and it hence accounts for the same periodic orbits. Thus, this version of the Battle of the Sexes has the same NE distribution as the Chicken game.

Now, when we apply Eisert's quantization protocol and construct the 2-dimensional map similar to that discussed for the quantum Prisoner's dilemma, we unexpectedly find that we do not need any longer to consider the space of strategies S. Specifically, the space of strategies given by

$$S' = \{U(\theta,\phi)| -\pi \leq \theta \leq \pi \text{ and } 0 \leq \phi \leq \pi/2\} \tag{29}$$

proves now to be the smallest set which guaranties the endomorphic property of the map. This fact is demonstrated in Figure 8. In the left panel we iterate ϕ-lines in the upper semiplane (solid lines). We observe that the whole upper semiplane is mapped into the lower semiplane (dashed curves), which in turn is mapped again into the upper semiplane (dotted curves). That means that the mapping procedure perfectly works when restricted to this space. In addition, we conclude from Figure 8 that the map we are exploring does not account for fixed points. Moreover, restricting our analysis to the upper semiplane, we identify one possible

---

[6] To make the comparison easier to follow, we keep 'C' and 'D' to label the strategies, instead of the usual 'O' and 'T' (for 'Opera' and 'TV', respectively).
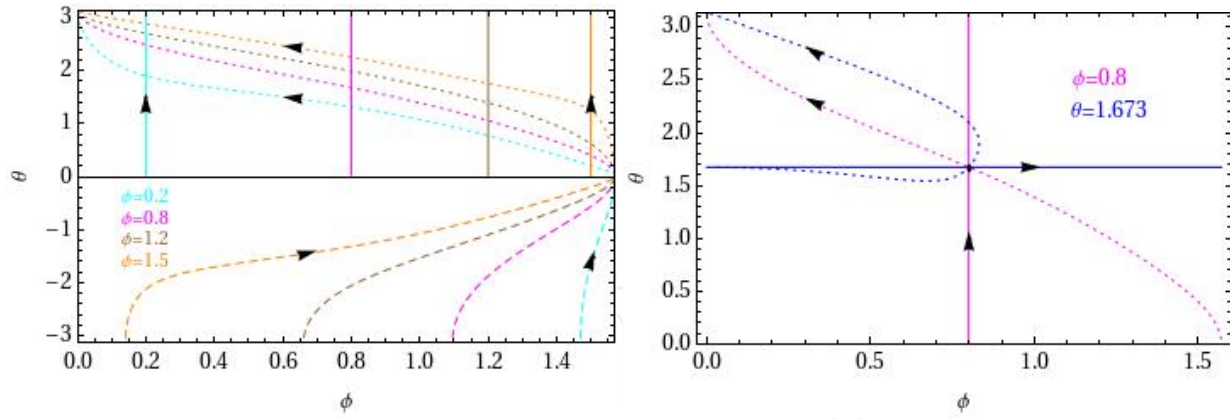
Figure 8. Maximization map associated to the quantum symmetrized Battle of the Sexes game. Left: for the upper semiplane, the first and second iterations (dashed and dotted curves, respectively) of the constant ϕ lines (solid lines). Right: Second iterations of the lines $\phi = 0.8$ (for $\theta > 0$) and $\theta = 1.673$. See the text for the explanation.
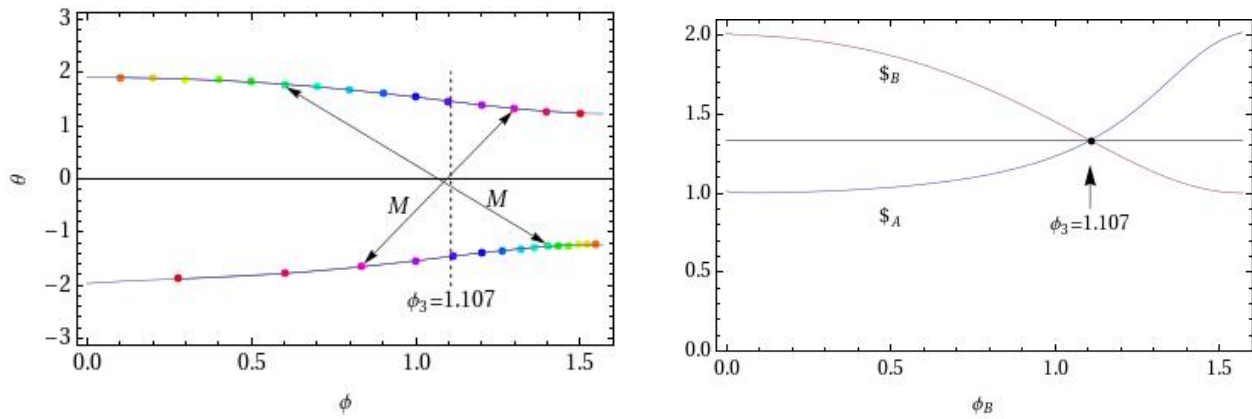

Figure 9. Left: Maximization map associated to the quantum symmetrized Battle of the Sexes game. Right: As a function of Alice's ϕ parameter, payoffs of Alice and Bob in the set of NE (see the text).

2-periodic point for each value of the parameter ϕ, namely, the point where each dotted curve intersects the corresponding solid line. To test whether these candidates actually represent 2-periodic points, we peak the values of the parameter θ where the intersections occur and iterate the squared map for these values of θ in the whole range of ϕ. In the right panel of Figure 8 we show this procedure for $\phi = 0.8$. The double intersection shows that our candidates iterate (under M^2) in points with the same coordinate θ, being hence fixed points of the squared map. As a conclusion, we find a continuous set of primitive 2-periodic orbits. Each orbit in this set is composed by one point in the upper semiplane and a second point in the lower semiplane. Left panel of Figure 9 depicts the organization of the orbits in the set, within the analysis discussed so far[7]. The two members of each cycle are located in two branches symmetric under a reflection around $\theta = 0$, however the correspondence between both members is not simply given by an inversion of the parameter θ, but that related to the colored points in the graph (such colored points were selected to be equidistant in the upper branch). Yet, for the specific value $\phi_3 = 1.107$, the two members are actually symmetrically located, having coordinates $\phi = \phi_3, \theta = \theta_3$ and $\phi = \phi_3, \theta = -\theta_3$, with $\theta_3 = 1.4596$.

---

[7] As the map is symmetric under a reflection around $\theta = 0$, the iteration of the lower semiplane gives rise to the same outcome to that depicted in Figure 9.

Now, as each periodic orbit can be parametrized by its ϕ coordinate associated to the member in the upper branch, we can come to the quantum game problem and study the NE as this parameter is varied. Right panel of Figure 9 shows the payoffs of Alice and Bob for each NE in the set, as a function of Alice's ϕ parameter (in the upper branch). It is interesting to observe that the outcomes $\phi_1 = 0$, $\theta_1 = 1.9$ and $\phi_2 = \pi/2$, $\theta_2 = -1.24$ play a role similar to that of the strategies C and D in the classical game. Namely, if for example Alice plays $\hat{S}_1 = \hat{U}(\theta_1, \phi_1)$ and Bob plays $\hat{S}_2 = \hat{U}(\theta_2, \phi_2)$, they receive the payoffs $\$_A = 1$ and $\$_B = 2$. Nevertheless, in the present scenario the joined strategy '$\hat{S}_1 - \hat{S}_2$' does fulfill the NE conditions, whereas '$\hat{C} - \hat{D}$' does not. Of course, if we plotted the payoff functions as a function of Bob's ϕ parameter in the upper branch, the conclusions would be symmetrical under the interchange of $\hat{S}_1$ and $\hat{S}_2$ (the same way as an interchange of C and D accounts for a second NE in the classical game, with the payoffs inverted). However, an interchange of the strategies is not the only way to invert the payoffs of the parties. From Figure 9 it turns out that the strategies $\hat{S}_{-1} = \hat{U}(-\theta_1, \phi_1)$ and $\hat{S}_{-2} = \hat{U}(-\theta_2, \phi_2)$ give $\$_A(\hat{S}_{-2}, \hat{S}_{-1}) = 2$ and $\$_B(\hat{S}_{-2}, \hat{S}_{-1}) = 1$, so '$\hat{S}_{-1} - \hat{S}_{-2}$' and '$\hat{S}_{-2} - \hat{S}_{-1}$' represent a second pair of 2-cycle NE with exactly the same characteristics of '$\hat{S}_1 - \hat{S}_2$' and '$\hat{S}_2 - \hat{S}_1$'. Nevertheless, the most interesting feature of the game concerns the emergence of a very special NE given by the strategies $\hat{S}_3 = \hat{U}(\theta_3, \phi_3)$ and $\hat{S}_{-3} = \hat{U}(-\theta_3, \phi_3)$. The joined strategies '$\hat{S}_3 - \hat{S}_{-3}$' and '$\hat{S}_{-3} - \hat{S}_3$' give both players the same payoff $\$_A = \$_B = 4/3$, and are not comparable to some outcome of the classical game. In the classical game we saw that the mixed joined strategy $(p, q) = (2/3, 2/3)$ fulfills the NE conditions, however this NE accounts for a payoff $\bar{\$}_A = \bar{\$}_B = 2/3$, even worse than the lower payoff given by the pure-strategy NE. '$\hat{S}_3 - \hat{S}_{-3}$' and '$\hat{S}_{-3} - \hat{S}_3$', instead, are joined strategies from which players can not increase their payoffs without lessening that of the other party, being therefore PO outcomes of the game. Accordingly, this version of the symmetrized Battle of the Sex game accounts for 2 possible optimal solutions which prevent players from facing with the classical conflict.

Finally, we observe that when restricted to the set of strategies given by Eisert et al. there are no periodic points surviving in the map domain. That means that in the original space of strategies there are no NE. Namely, for any possible decision of Alice, Bob can find a convenient counter-strategy which places Alice in a situation from which she would prefer to deviate.

From the previous discussion, we observe again an interesting fact from the comparison of two games. When we compare the Chicken and the symmetrized Battle of the Sexes, we see that both games display the same NE distribution at the classical level, however they are totally different when the periodic points method is applied to identify NE in the extended space of quantum strategies. From this comparison and that established between the Prisoner's dilemma and the Chicken game we conclude that from the classical game it is not possible to predict a priori what is going to happen at the quantum level, and that from the quantum behavior it is not possible to unambiguously infer the classical substrate of the game. Of course, the NE distribution does not completely defines the category of a game (see [19]).

4.3. Connections between Eisert's games

As we established above, the maps corresponding to the quantum Prisoner's dilemma and the quantum Chicken game are topological equivalent. For $a = \$_A(C, C)$, $b = \$_A(C, D)$,

$c = \$_A(D, C)$ and $d = \$_A(D, D)$, this fact can be explicitly stated by considering the function

$$f(a, b, c) = \frac{1}{2} \arccos \left[\frac{2a - b - c}{c - b} \right],$$ (30)

which gives the parameter $\tilde{\phi}$ limiting the region where the $\tilde{\phi}$-lines are iterated (see Figure 4). By changing the value of b we only stretch or shrink that region, but whenever $\tilde{\phi}$ ranges in the interval $(0, \pi/2)$, we do not modify the topological structure of the map. For $a = 3$ and $c = 5$, $\tilde{\phi}$ can escape this interval only if $b \geq 3$, but this would contradict the conditions of the Prisoner's dilemma ($b < d < a < c$) and the Chicken game ($d < b < a < c$). The transition between the two games happens at $b = 1$ ($\tilde{\phi} = \pi/4$), for which the map still preserves the same characteristics[8].

On the other hand, the comparison of the Chicken game and the simmetrized battle of the Sexes game reveals an other interesting feature. This time, we have two games with exactly the same classical ingredients (even when mixed strategies are allowed), but with completely different behaviors at the quantum level. The most surprising thing concerns the symmetrized Battle of the Sexes game, which when studied within Eisert's protocol displays not only a very rich distribution of NE (two of these off-diagonal NE fulfilling the PO condition as well), but also a different domain for the associated map. This intriguing result forces us to establish a connection in terms of geometrical arguments, as we did when compared the Prisoner's dilemma and the Chicken game. To pursue this task, let start by considering the following game

	Bob: C	Bob: D
Alice: C	(3, 3)	(2, 5)
Alice: D	(5, 2)	(3, 3)

This game, having not much interest from the classical point of view, when quantized has exactly the same behavior as the Prisoner's dilemma and the Chicken game. Moreover, as it differs from the Chicken in the entry d only, it has the same value for the parameter $\tilde{\phi}$ and thus an associated map which is a copy of that of the quantum Chicken game.

Now, when b starts increasing, the regions where the iterations (dashed and doted curves in Figure 4) are located shrink, and eventually they collapse (as the threshold given by $b = 3$ is reached) to the edges $\phi = \pm\pi/2$ (which are connected in a Möbius strip fashion, according to the projective plane topology). For $b > 3$, $\tilde{\phi}$ ceases to be real, which means that the map can not behave anymore in the same fashion. If we rewrite the table for any value of $b > 3$, we obtain the conditions of the symmetrized Battle of the Sex game ($a = d < b < c$), and an associated map which is topological equivalent to that of Figure 8 (curves in both maps are related by means of smooth deformations). In terms of nonlinear dynamic language, we are here in presence of a bifurcation of codimension 1, the entry b in the payoff matrix being the bifurcation parameter. In our example, when $b < 3$ we have a class of quantum games whose associated map displays (even when they can be different classically) a topological equivalence. However, when $b > 3$ the structure of the maps associated to the quantum game changes abruptly, giving rise to a more complex class of maps. Moreover, within the latter class, each side of the projective plane accounts for an endomorphism on its own (which is a

---

[8] We chose standard values to present the games. However, the conclusions outlined here are independent of the specific choice.

symmetric repetition of the other endomorphism), a fact that allows us to define the map in just a half piece of the initial domain.

5. A geometrical classification of Eisert's games

The discussion of the previous section allows us to formulate new questions. If we compute the number of different bi-matrices which can be constructed with at least 3 different entries, we find that there are 54 2×2 possible games which can be analyzed according to our procedure. However, we saw that some quantum games can be connected by means of geometrical considerations, and grouped in classes according to the topological structure of the associated maps. It is therefore natural to ask how many classes can be obtained under this classification scheme[9]. Here we only summarizes the main results of the classification scheme and establish, for the most famous examples, to which class each game belongs. For a full description of the the subject see [22].

Class 1 comprises two subclasses. The games in these subclasses are enumerated in table 4. Class 1a includes the Prisoner's dilemma (game 2) and the Chicken game (game 3). The maps within this class are defined on the projective plane (space of strategies S). In both subclasses points of period 2 are located at $\theta = 0$. Specifically, the maps belonging to class 1a have its periodic points at $\theta = 0$ and $\tilde{\phi} \leq |\phi| \leq \pi/2$ whereas those of class 1b have its periodic points at $\theta = 0$ and $0 \leq |\phi| \leq \tilde{\phi}$.

	Class 1a		Class 1b
1	$b = d < a < c$	5	$c = d < a < b$
2	$b < d < a < c$	6	$c < d < a < b$
3	$d < b < a < c$	7	$d < c < a < b$
4	$b < a = d < c$	8	$c < a = d < b$

Table 4. Games of Class 1.

Games belonging to class 2 are enumerated in table 2. They include the well known Deadlock game (game 10). The associated map is defined in the space of strategies

$$S''' = \{U(\theta, \phi) | \ 0 \leq \theta \leq \pi \ \text{and} \ 0 \leq \phi \leq \pi/2\}$$

an is simply given by the expression

$$M(\theta, \phi) = (\theta, \pi/2 - \phi).$$

Accordingly, every second iteration is located on the ϕ-line which is iterated. This makes every point in the space of strategies a member of an orbit of period 2 whose second member is obtained by reflecting on the line $\phi = \pi/4$. Points with coordinate $\phi = \pi/4$ are thus the fixed points of the map.

Class 3 comprises two subclasses each composed by a single game. The games are enumerated in table 3. Being the maps defined in the projective plane, periodic points in both classes are located in the region $\tilde{\phi} \leq \phi \leq \pi/2 - \tilde{\phi}$, for

$$\tilde{\phi} \equiv \frac{1}{2} \arccos \left[\frac{b + c - \max\{a, d\}}{b - c} \right]. \tag{31}$$

---

[9] We stress that this classification relies on the geometrical properties of the map associated to the game, so it needs to be differentiate from other existing classification schemes for games (see [19] for a discussion of this subject).

9	$b < a < c = d$	15	$a < c < b = d$	21	$b = a < c < d$
10	$b < a < c < d$	16	$a < c < b < d$	22	$c = a < b < d$
11	$c < a < b = d$	17	$b < c < a = d$	23	$b < a = c < d$
12	$c < a < b < d$	18	$b < c < a < d$	24	$c < a = b < d$
13	$a < b < c = d$	19	$c < b < a = d$	25	$a = b < d < c$
14	$a < b < c < d$	20	$c < b < a < d$	26	$a = c < d < b$

Table 5. Games of Class 2.

Any of these points is a member of an orbit of period 2 whose second member is given by a reflection on the line $\phi = \pi/4$. In this class, the periodic orbits are symmetric under a reflection on the θ axis.

	Class 3a		Class 3b
27	$b < a < d < c$	28	$c < a < d < b$

Table 6. Games of Class 3.

The two subclasses comprised by class 4 are enumerated in table 7. Class 4a includes the symmetrzed Battle of the Sexes (game 29). The behavior of the map and the location of the periodic orbits was explained above for the symmetrzed battle of the Sexes. For class 4b the picture is the same as for class 4a after a reflexion around the axis $\phi = \pi/4$, so the same symmetry holds for the periodic orbits.

	Class 4a		Class 4b
29	$a = d < b < c$	33	$a = d < c < b$
30	$a < d < b < c$	34	$a < d < c < b$
31	$d < a < b < c$	35	$d < a < c < b$
32	$a < b = d < c$	36	$a < c = d < b$

Table 7. Games of Class 4.

Games included in class 5 are enumerated in table 8. They are divided in 2 subclasses with a single member each, and have an associated map defined in the space of strategies of the symmetrized Battle of the Sexes game (space of strategies S'). NE are of two different types in each subclass. For class 5a, NE are of the same type as in class 4a for $\phi < \tilde{\phi}$, and as those of class 2 for $\phi > \tilde{\phi}$, whereas for games in class 5b NE are as those of class 4b for $\phi > \tilde{\phi}$ and as those of class 2 for $\phi < \tilde{\phi}$. $\tilde{\phi}$ is given in equation 31.

	Class 5a		Class 5b
37	$a < b < d < c$	38	$a < c < d < b$

Table 8. Games of Class 5.

Games belonging to class 6 are enumerated in table 9. Again, the games are separated in two subclasses, corresponding to two different maps. Class 6a includes the so called Stag Hunt game (games 41 and 42). The associated map, for both subclasses, is defined in the projective plane, and the periodic orbits are located in the axis $\theta = 0$, with no restrictions in the coordinate ϕ.

	Class 6a			Class 6b
39	$d = b < c < a$		46	$d = c < b < a$
40	$d < b < c < a$		47	$d < c < b < a$
41	$b < d < c < a$		48	$c < d < b < a$
42	$b < c = d < a$		49	$c < b = d < a$
43	$b < c < d < a$		50	$c < b < d < a$
44	$b < d < a = c$		51	$c < d < a = b$
45	$d < b < a = c$		52	$d < c < a = b$

Table 9. Games of Class 6.

Games belonging to class 7 are enumerated in table 10. Again, the games are separated in two subclasses, corresponding to two different maps. These maps have a curious behavior. Being defined in the projective plane, the map corresponding to class 7a maps all the domain into the line $\phi = \pi/2$, which is in turn mapped into the point $\theta = \pi/2$, $\phi = 2$. Therefore, Eisert's joined strategy '$\hat{Q} - \hat{Q}$' represents the sole NE of this game. The map corresponding to the class 7b, in turn, maps all the projective plane in the axis $\phi = 0$, which in turn is mapped into the origin. The sole NE of the latter game is thus represented by the joined strategy '$C - C$' of the classical game.

	Class 7a			Class 7b
53	$d < a = b < c$		54	$d < a = c < b$

Table 10. Games of Class 7.

6. Conclusions

After introducing Eisert's theory for quantizing games, we analyzed a periodic point-based procedure designed to identify NE in 2×2 quantum games defined on an extended set of strategies. According to our analysis, NE of Eisert's 2-parameter quantum Prisoner's dilemma are located on a segment of a projective plane equator (points with $\theta = 0$, excluding those for which $|\phi| < \tilde{\phi}$). All strategies fulfilling the NE condition are 2-cycle NE except that corresponding to $\phi = \pi/2$. The latter strategy corresponds to Eisert's operator $\hat{Q}$, and it is actually the only strategy which survives if we restrict ourselves to the original set defined in [5]. Now, as $\$_A(0, \phi', 0, \phi'') = 3\cos(\phi' + \phi'') + \sin((\phi' + \phi''))$, it turns out that

$$\$_A(\hat{R}_\pm, \hat{R}_\mp) = 3 \quad \forall \alpha \in [0, \pi/2].$$

Hence, we conclude that all joined strategies '$\hat{R}_+ - \hat{R}_-$' and '$\hat{R}_- - \hat{R}_+$' with $\tilde{\phi} \leq \alpha < \pi/2$ are NE as good as the '$\hat{Q} - \hat{Q}$' one (in the sense of the payoff given to the players). However, in the scenario of the extended strategy set the players have not an obvious choice as they have in the restricted case. This is the reason why Eisert et al. designed a protocol with such a special (somehow artificial) set. Nevertheless, as it is discussed in [1] and [8], the set of strategies adopted in [5] and its corresponding outcome are far from general. Motivated by this fact, we adopted here an alternative but still valid set which was the only one which proved to be suitable for developing the periodic point procedure. Yet, at the end of section 3 we discuss a possible modification of the story behind the game which has not effects on the original quantum game (not even at the classical level), but that makes the new NE be as suitable as the result obtained by Eisert et al.

In section 4 we considered the Chicken game and a symmetrized version of the Battle of the Sexes. As a conclusion of the comparison of this two examples and the Prisoner's dilemma, we observed that the outcome of the quantization procedure has no reminiscences with the classical nature of the game. Specifically, at the classical level the Prisoner's dilemma and the Chicken game display a different NE distribution. In the first case there is just one NE represented by the joined strategy 'defect-defect', whereas in the second case the NE correspond to 'cooperate-defect' and 'defect-cooperate'. Nevertheless, when analyzed within the framework of Eisert's protocol, both games share exactly the same behavior, namely, the continuous set of NE given by the joined strategies '$\hat{R}_+ - \hat{R}_-$' (for $\tilde{\phi} \leq \alpha < \pi/2$) which in addition fulfill the PO condition (being therefore rational solutions of the game). On the contrary, after comparing the Chicken game and the simmetrized Battle of the Sexes, we conclude that games having the same NE distribution at the classical level, can behave in a completely different fashion when Eisert's scheme is implemented in the extended space of strategies.

In section 4.3 we showed that games having different behaviors at the quantum level, can actually be related through bifurcations for maps. Moreover, we demonstrated that the bifurcation parameter is directly obtained from the bi-matrix defining the classical game. In section 5, we grouped every 2×2 games in classes according to the map which is associated to the quantum game, and showed that the number of classes is certainly small. It is therefore natural to ask how all games (or the classes representing them) connect by means of a specific bifurcation. Namely, which are the entries in the payoff matrices which play the role of the bifurcation parameter for any two, arbitrary, games. Or whether it is necessary, to connect two classes through a bifurcation, to include a third one as an intermediate class in the path. This would make it necessary to consider two different entries to account for the bifurcation, changing therefore the bifurcation codimension and making the picture a little more complicated but more interesting. These issues will be addressed in a future work.

Author details

David Schneider
Universidade Estadual de Campinas, Brazil

7. References

[1] Benjamin, S. C. & Heyden, P. M. [2001a]. Comments on "quantum games and quantum strategies, *Phys. Rev. Lett.* 87: 069801–1.

[2] Benjamin, S. C. & Heyden, P. M. [2001b]. Multiplayer quantum games, *Physical Review A* 64: 030301.

[3] Chen, L., Ang, H., Kiang, D., Kwek, L. C. & Lo, C. [2003]. Quantum prisoner dilemma under decoherence, *Physics Letters A* 316: 317–323.

[4] Du, J., Li, H., Xu, X., Shi, M., Wu, J., Zhow, X. & Han, R. [2001]. Entanglement playing a dominating role in quantum games, *Physics Letters A* 289: 9–15.

[5] Eisert, J., Wilkens, M. & M.Lowenstein [1999]. Quantum games and quantum strategies, *Phys. Rev. Lett.* 83: 3077–3080.

[6] Flitney, A. P. & Abbot, D. [2004]. Quantum two and three person duels, *J. Opt. B* 6: S860–6.

[7] Flitney, A. P. & Abbot, D. [2005]. Multiplayer quantum minority game with decoherence, *J. Phys. A: Math. Gen.* 38: 449.

[8] Flitney, A. P. & Hollenberg, L. C. L. [2007]. Nash equilibria in quantum games with generalized two-parameters strategies, *Physics Letters A* 363: 381–388.

[9] H. Guo, J. Z. & Koehler, G. [2008]. A survey of quantum games, *Decis. Support Syst.* 46: 318–332.

[10] Hidalgo, E. G. [2008]. Quantum games and the relationships between quantum mechanics and game theory, *arXiv:0803.0292v1 [quant-ph]* .

[11] Iqbal, A. & Toor, A. H. [2001a]. Entanglement and dynamic stability of nash equilibria in a symmetric quantum game, *Physics Letters A* 286: 245–250.

[12] Iqbal, A. & Toor, A. H. [2001b]. Evolutionarily stable strategies in quantum games, *Physics Letters A* 280: 249–256.

[13] Iqbal, A. & Toor, A. H. [2002]. Quantum mechanics gives stability to a nash equilibrium, *Physical Review A* 65: 022306.

[14] Massey, W. S. [1977]. *Algebraic Topology: An Introduction*, Springer-Verlag, New York.

[15] Meyer, D. [1999]. Quantum strategies, *Phys. Rev. Lett.* 82: 1052–1055.

[16] Nawaz, A. & Toor, A. H. [2006]. Quantum games with correlated noise, *J. Phys. A: Math. Gen.* 39: 9321.

[17] Piotrowski, E. W. & Sladkowski, J. [2002]. Quantum market games, *Phyisica A* 312: 208–216.

[18] Ramzan, M. & Khan, M. K. [2009]. Noise effects in a three-player prisoner's dilemma quantum game, *J. Phys. A: Math. Gen.* 41: 435302 (11pp).

[19] Rosero, A. F. H. [n.d.]. *Classification of Quantum symmetric Nonzero-sum* 2×2 *games in the Eisert's Scheme*, arXiv:quant-ph/0402117v2.

[20] Schneider, D. M. [2011]. A periodic point-based method for the analysis of nash equilibria in 2×2 symmetric quantum games, *J. Phys. A: Math. Theor.* 44: 905301.

[21] Schneider, D. M. [2012]. A new geometrical approach to nash equilibria organization in eisert's quantum games, *J. Phys. A: Math. Theor.* 45: 085303.

[22] Schneider, D. M. [n.d.]. Geometrical-besed classification of eisert's quantum games, In preparation.

[23] Stohler, M. & E.Fischbach [2005]. Non-transitive quantum games, *Fizika B* 14: 235–244.

[24] Werner, R. F. [1998]. Optimal cloning of pure states, *Phys. Rev. A* 58: 1827.